

# Anti-Corrosion Performance of Cr<sup>+6</sup>-Free Passivating Layers Applied on Electrogalvanized

Célia Regina Tomachuk<sup>1</sup>, Alejandro Ramón Di Sarli<sup>2</sup>, Cecilia Inés Elsner<sup>2</sup>

<sup>1</sup>Energy and Nuclear Research Institute, IPEN/CNEN-SP, CCTM, Av. Prof. Lineu Prestes, São Paulo, Brazil; <sup>2</sup>CIDEPINT: Research and Development Center in Paint Technology (CICPBA-CONICET), Av.52 s/n entre 121 y 122. CP. B1900AYB, La Plata-Argentina.  
Email: tomazuk@gmail.com, direccion@cidepint.gov.ar

Received April 29<sup>th</sup>, 2010; July 22<sup>nd</sup>, 2010; August 4<sup>th</sup>, 2010.

## ABSTRACT

Hexavalent chromium-based passivation treatments have been successfully used as promoters of conversion coatings for many years. Their effectiveness is without question although there are many problems with regard to their environmental suitability. Hexavalent chromium compounds are carcinogenic and toxic. These problems have lead researchers to evaluate other potential systems, with lower toxicity, to ascertain if they can replace chromates as effective passivators. Researchers have proposed several alternative passivation treatments; these are processes based on molybdates, permanganates, titanates, rare earth metal and Cr<sup>3+</sup> (considered to be non-carcinogenic) compounds. In this work, zinc coatings obtained from free-cyanide alkaline bath and submitted to a Cr<sup>3+</sup> based passivation treatment with different colors were studied. The corrosion behavior was studied by polarization measurements and mainly by electrochemical impedance spectroscopy in 0.6 N NaCl solution. Morphological observations on the coatings surface were also performed. The results indicate that the green-colored Cr<sup>3+</sup> passivated coatings have a good corrosion resistance followed by yellow and blue-colored passivation respectively. They could be a less polluting alternative to the traditional chromated coatings.

**Keywords:** Zinc, Conversion Treatment, Impedance Spectroscopy, Salt Spray, Corrosion

## 1. Introduction

Electroplated zinc coating is employed as active galvanic protection for steel. However, as the zinc is an electrochemically highly reactive metal, its corrosion rate may be also high in indoor but particularly under outdoor exposure conditions [1]. For this reason, it is necessary a post treatment in order to increase the lifetime of zinc coatings. In current industrial practice, this treatment consists of immersion in a chemical bath that forms a conversion layer on plated zinc. This latter layer is a dielectric passive layer with high corrosion resistance and is also a better surface for paint adherence. The main problem of traditionally used post treatments is the presence of Cr<sup>6+</sup> salts, considered carcinogenic substances which usage is forbidden by European norms [2]. Responding to increasingly more rigorous environmental protection activities, recent years have shown progressive advances in order to reduce the use of environmentally-hazardous materials. In line with this purpose, the development of various kinds of chromate-free coated

steel sheets, to be used in food, automotive, appliances, etc. industries, is being extensively explored all over the world. In this sense, the most common transitional alternative to Cr<sup>6+</sup> is Cr<sup>3+</sup>, which is used since the mid 1970's [3-9]. According to Fonte *et al.* [10], the Cr<sup>3+</sup> conversion layer formed in a bath containing transition metal ions such as Co<sup>2+</sup>, Ni<sup>2+</sup> and Fe<sup>2+</sup> showed higher corrosion resistance than those formed in a bath without transition metal ions. This finding was confirmed by Tomachuk *et al.* [11,12].

Molybdates, tungstates, permanganates and vanadates, including chromium like elements, were the first chemical elements tried as hexavalent chromium substitutes [13-17]. Recently many alternative coatings were developed based on zirconium and titanium salts [18-20], cobalt salts [21,22], organic polymers [23,24] and rare earth salts [25]. However, preparation and corrosion behavior of these coatings is not clear and their practical usage is doubtful.

In order to find an alternative treatment to Cr<sup>6+</sup> con-

version coating, several treatments that present a good anti-corrosive behavior, a high benefit/cost relation and, mainly, low environmental impact are still to be developed. Usually, the corrosion behavior of coatings is evaluated using traditional tests such as Salt Spray [26], Kesternich test [27], saturated humidity [28]. However the authors consider important the application of electrochemical methods to obtain fast information about the corrosion reactions kinetics.

Among the electrochemical techniques that can be used, the electrochemical impedance spectroscopy (EIS) was selected based on the already obtained results for metal and metal-coated corrosion evaluation [29-32].

The main purpose of the present work was to find an environmentally friendly conversion treatment able to replace satisfactorily those passivating ones based on Cr<sup>6+</sup>. Electrogalvanized steel covered with Cr<sup>6+</sup>-free passivating layers were investigated using AC and DC electrochemical techniques. Morphological studies of the coatings surface were also performed.

## 2. Experimental Details

### 2.1. Samples Preparation

Electrogalvanized steel samples (7.5 × 10 × 0.1 cm) were industrially produced and covered with the following conversion treatments: 1) blue-colored Cr<sup>3+</sup> based passivation; 2) yellow-colored Cr<sup>3+</sup> based passivation; 3) green-colored Cr<sup>3+</sup> based passivation. For each conversion layer, an individual commercial conversion bath was formulated and the coating was produced according to the respective supplier recommendations.

### 2.2. Thickness Measurements

The coatings thickness was measured using the Helmut Fischer equipment DUALSCOPE MP4.

### 2.3. Morphology

The coatings morphology was determined from scanning electron microscopy (SEM) analyses using a LEICA S440 microscope.

### 2.4. Electrochemical Behavior

The electrochemical cell consisted of a classic three-electrode arrangement, where the counter electrode was a platinum sheet, the reference one a saturated calomel electrode (SCE) and the working electrode each coated steel sample with a defined area of 7 cm<sup>2</sup>. All measurements were performed at a constant room temperature (22 ± 3 °C) in 0.6 N NaCl solution.

Potentiodynamic polarization experiments were carried out using a Solartron 1280 electrochemical system at a swept rate of 1 mV.s<sup>-1</sup>, over the range ±0.300 V(SCE)

from the open-circuit potential OCP). Before each swept, the electrode in contact with the electrolyte was stabilized for several minutes. The corrosion current density (*j*) and corrosion potential (*E*<sub>corr</sub>) were obtained from a Tafel slope by extrapolation of the linear portion of anodic and cathodic branches.

Impedance spectra in the frequency range 2.10<sup>-2</sup> Hz < *f* < 4.10<sup>4</sup> Hz were performed in the potentiostatic mode at the OCP, and as a function of the exposure time in the electrolyte solution, using a Solartron 1260 Frequency Response Analyzer (FRA) coupled to a Solartron 1286 electrochemical interface (EI). The amplitude of the applied AC voltage was 3 mV peak to peak. Each sample's surface evolution was analyzed until white corrosion products could be seen by the naked eye. The experimental spectra were interpreted on the basis of equivalent electrical circuits' models using the ZView fitting software by Scribner Associates. All impedance measurements were carried out by triplicate in a Faraday cage in order to minimize external interference on the system studied.

## 3. Results and Discussion

The overall coating thickness and description of the samples investigated in this work are reported in **Table 1**. In it can be seen that these showed similar and uniform thickness; besides, they also exhibited a bright appearance throughout their extension. Unfortunately, information related with the passive layer thickness was not possible to be obtained.

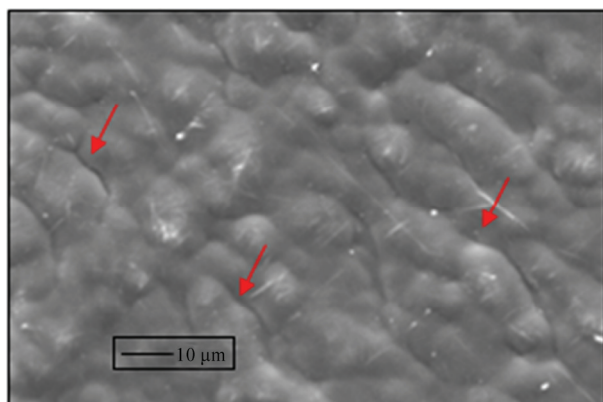
### 3.1. Morphology

The consideration of the coating morphology after the coating/drying process is very important since the presence of flaws such as pores and/or other defects could be areas where localized corrosion of the treated zinc surface starts from its exposure to a given environment [33]. Therefore, after applying the conversion treatment, the coatings surface morphology was observed up to 1,000X

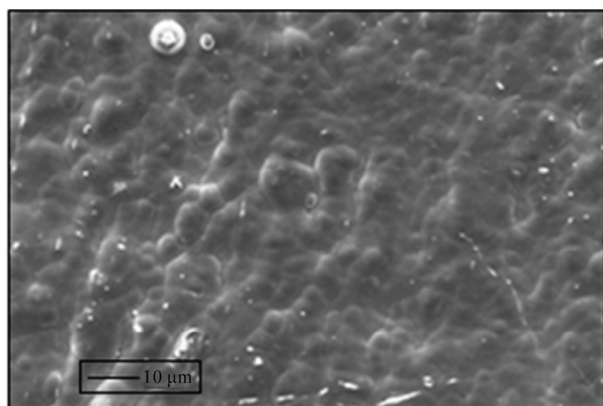
**Table 1. Characteristics of the samples.**

| Identification | Description   | Thickness<br>(Zn + conversion<br>treatment)<br>(µm) |
|----------------|---|---|
| A              | blue-colored Cr <sup>3+</sup><br>passivation UniFix Zn-3-50<br>(LABRITS®) | 10.8  |
| B              | yellow-colored Cr <sup>3+</sup><br>passivation UniYellow 3<br>(LABRITS®)  | 11.2  |
| C              | green-colored Cr <sup>3+</sup><br>passivation SurTec S680®                | 10.4  |

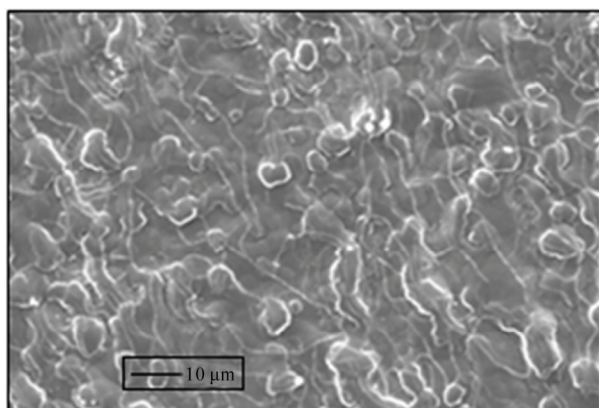
by SEM (Figure 1). All the samples presented surface roughness. Besides, A samples, subjected to blue-colored Cr<sup>3+</sup>-based passivation, exhibited surface fissures (indicated by the red arrows) which reduce its protective properties (Figure 1(a)), while the B samples, subjected to yellow-colored Cr<sup>3+</sup>-based passivation, exhibited homogenous structure with nodular growth (Figure 1(b)),



(a)



(b)



(c)

Figure 1. Microstructure of the tested coatings. (a) sample A; (b) sample B; (c) sample C.

and C samples, subjected to green-colored Cr<sup>3+</sup> passivation, exhibited a gel-like structure (Figure 1(c)). The characteristic cracks of chromate coatings were not present, perhaps due to its thin thickness [34].

### 3.2. Polarization Curves

Potentiodynamic polarization curves were performed at a swept rate of a 1 mV.s<sup>-1</sup> in the range ±0.300 V (SCE) with respect to the OCP. This procedure has been repeated for all the investigated samples. Figure 2 shows typical potentiodynamic polarization curves for passivated electrogalvanized steel in chloride solution.

Corrosion potential,  $E_{\text{corr}}$ , and corrosion current density,  $j_{\text{corr}}$ , values obtained from Figure 2 were reported in Table 2. As it can be seen, the corrosion potential ( $E_{\text{corr}}$ ) of A samples was more negative, i.e. less noble, and this means that from the thermodynamic point of view these samples type are more susceptible to be corroded. With regard to B and C samples, both presented similar and more positive corrosion potential values than A samples, indicating that a corrosion resistance improvement took place, probably due to the homogenous morphology of the covering layer showed in Figures 1(b) and 1(c) provided a better barrier resistance.

On the other hand, the corrosion current density ( $j_{\text{corr}}$ ) of C samples is one order of magnitude less than the corresponding to the other two sample types tested, i.e.,

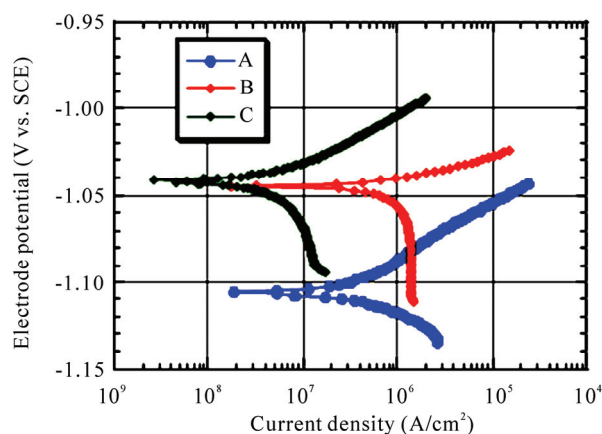


Figure 2. Polarization curves of the samples tested in 0.6 N NaCl solution,  $v = 1$  mV/s.

Table 2.  $E_{\text{corr}}$  and  $j_{\text{corr}}$  values of Zn coatings after applying the conversion treatment.

| Conversion Treatment | $E_{\text{corr}}$ V(SCE) | $j_{\text{corr}}$ $\mu\text{A}/\text{cm}^2$ |
|----------------------|--------------------------|---|
| A                    | -1.10                    | 0.2   |
| B                    | -1.04                    | 0.4   |
| C                    | -1.04                    | 0.02  |

its corrosion rate is lower.

### 3.3. Electrochemical Impedance Spectroscopy

EIS measurements carried out in the 0.6 N NaCl solution were discontinued upon the white corrosion products on the surface could be seen by naked eye.

**Figure 3** shows a Nyquist representation of the time dependent electrochemical impedance, while **Figure 4** illustrates the electrical equivalent circuits able of simulating the physicochemical processes taking place at the coated steel surface. It is important to emphasize that experimental impedance data obtained for **A** and **B** samples were analyzed on the basis of the electric equivalent circuit depicted in **Figure 4(a)**, while for the **C** samples was used the shown in **Figure 4(b)** [35]. In these figures,  $R_{sol}$  represents the electrolyte resistance between the reference and working (coated steel) electrodes; the first time constant ( $R1Q1$ ) - where  $R1$  and ( $Q1 \equiv C1$ ) are respectively the resistance to the ionic flux and the dielectric capacitance of the conversion layer - appears at the higher frequencies. Once the permeating and corrosion-inducing chemicals (water, oxygen and ionic species) reach electrochemically active areas of the substrate, particularly at the bottom of the coating defects, the metallic corrosion becomes measurable so that its associated parameters, the charge transfer resistance,  $R2$ , and the electrochemical double layer capacitance, ( $Q2 \equiv C2$ ), can be estimated [3]. Sometimes, the  $Q2$  parameter can be associated to a diffusional process, which not only could be the rate-determining step (rds) of the corrosion reaction but also mask part of - or completely its time constant. It is important to remark that  $R2$  and  $C2$  values vary directly ( $R2$ ) and inversely ( $C2$ ) with the size of the electrochemically active metallic surface.

Distortions observed in these resistive-capacitive contributions indicate a deviation from the theoretical models in terms of a time constants distribution due to either lateral penetration of the electrolyte at the metal/coating interface (usually started at the base of intrinsic or artificial coating defects), underlying metallic surface heterogeneity (topological, chemical composition, surface energy) and/or diffusional processes that could take place along the test. Since all these factors cause the impedance/frequency relationship to be non-linear, they are taken into consideration by replacing one or more capacitive components ( $C_i$ ) of the equivalent circuit transfer function by the corresponding constant phase element  $Q_i$  (CPE), for which the impedance may be expressed as [36,37]:

$$Z = \frac{(j\omega)^{-n}}{Y_0}$$

where:

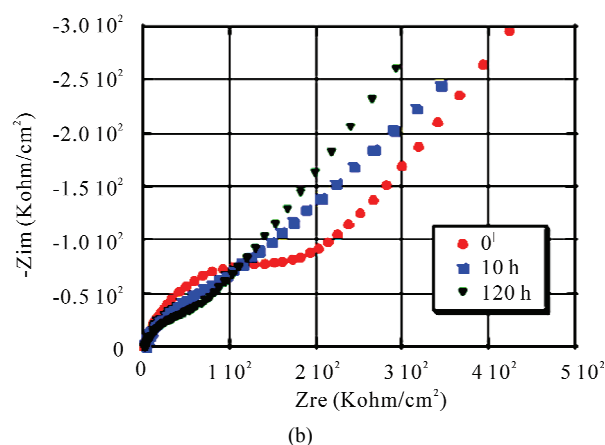
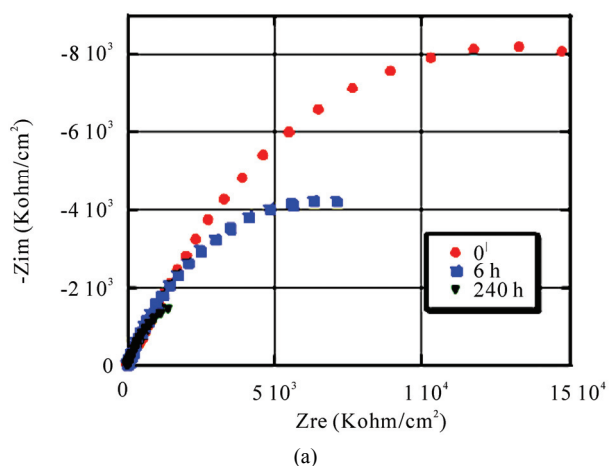


**Figure 3.** Evolution of the A and C samples impedance (Nyquist representation), (a) sample A; (b) sample C.

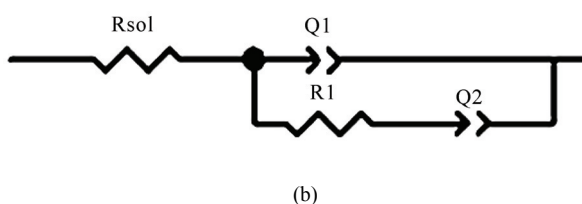
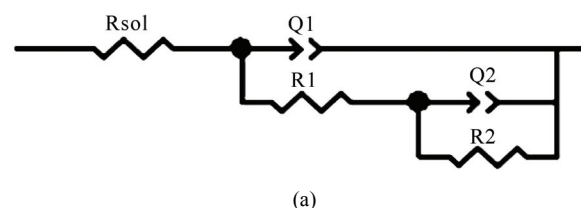


**Figure 4.** Equivalent circuit models used for fitting the impedance data.

$Z(\omega) \Rightarrow$  impedance of the CPE ( $Z = Z' + jZ''$ ) ( $\Omega$ )

$j \Rightarrow$  imaginary number ( $j^2 = -1$ )

$\omega \Rightarrow$  angular frequency (rad)

$n \Rightarrow$  CPE power: ( $n = \alpha/(\pi/2)$ )

$\alpha \Rightarrow$  constant phase angle of the CPE (rad)

$Y_0 \Rightarrow$  part of the CPE independent of the frequency ( $\Omega^{-1}$ )

Difficulties in providing an accurate physical description of the occurred processes are sometimes found. In such cases, a standard deviation value ( $\chi^2 < 10^{-4}$ ) between experimental and fitted impedance data may be used as final criterion to define the most probable circuit.

The comparison between simulated and experimental data at different exposure times are omitted for simplicity, however, in all cases, the experimental data were in good agreement with the model predictions.

The more interesting data to discuss are the exposure time dependent resistance **R1** of the passivation treatment (giving information on the barrier properties of the conversion layer) coupled in parallel with its **Q1** (related to the coating capacitance) and the charge transfer resistance **R2** (giving information on the kinetic of the corrosive process). These values, estimated from the fitting analysis of the impedance spectra, are reported in **Figures 5 to 7**, respectively.

**Figure 5** shows the trend of the parameter **R1**, which was associated to the evolution of the coating barrier properties and consequently with its degradation during exposure time in the aggressive aqueous solution. At zero time, the same and low **R1** values for **A** and **B** samples suggest poorer barrier properties when compared with the afforded by **C** samples. Then, it is observed a slight increase of the **R1** values until one hour of immersion for **C** samples and three hours for **A** and **B** samples. This was attributed to the blockage of the intrinsic and structural conversion layer defects with the soluble metallic

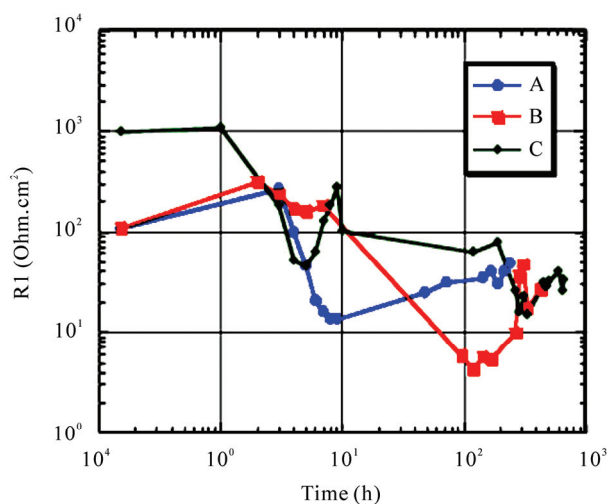
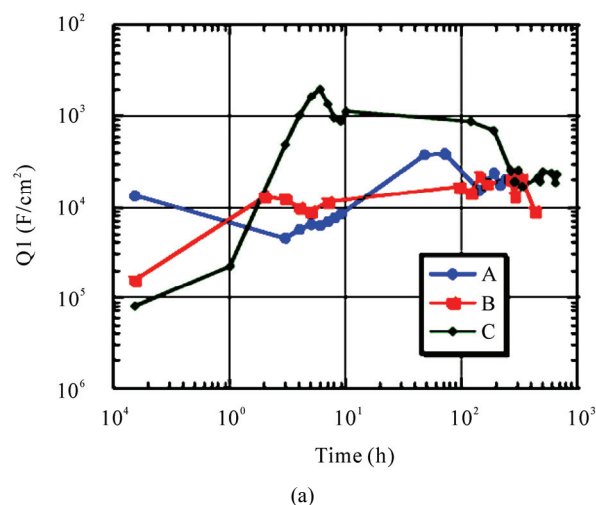
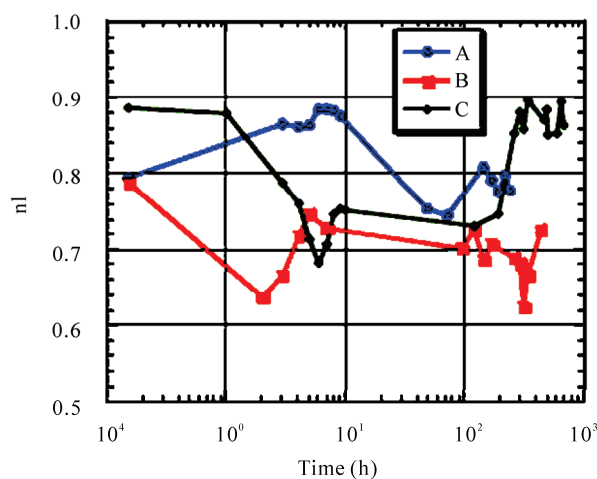


**Figure 5.** Values of **R1** as a function of immersion time in 0.6 N NaCl solution obtained from impedance data fitting for A, B and C samples.



(a)



(b)

**Figure 6.** Values of **Q1** and its exponent **n1** as a function of immersion time in 0.6 N NaCl solution obtained from impedance data fitting for A, B and C samples.

corrosion products formed due to the fast permeation of the corrosion inducing chemicals through the thin conversion layer. After that, these values started to decrease probably because of the interfacial corrosion reactions caused an increasing number and/or area of the coating defects and, consequently, of the exposed zinc area at the conversion layer/Zn interface. It is interesting to note that as the **R1** values decrease, the corresponding **Q1** increase (**Figure 6(a)**); such a behavior indicates that the involved relaxation process takes place at the same area [38]. At the end of the immersion test, an oscillating behavior with values less than the initial ones could be observed.

**Figures 6(a)** and **6(b)** show values of **Q1** and its exponent **n1** (see equation expressing the CPE definition) as a function of the immersion time in the 0.6 N NaCl

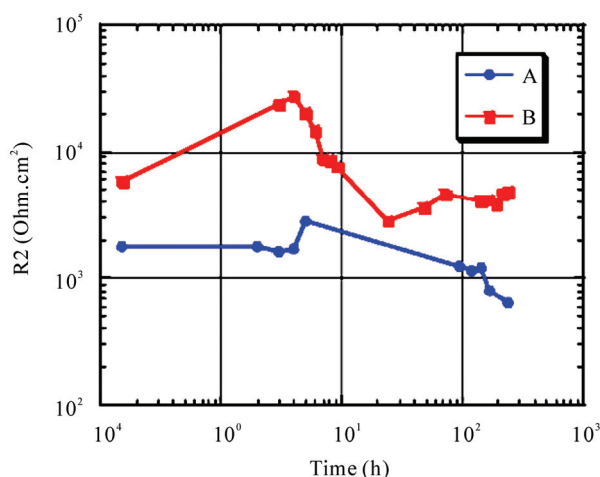


**Figure 7.**  $R_2$  as a function of immersion time in 0.6 N NaCl solution obtained from impedance data fitting for A and B samples.

solution. The initial conversion layer capacitance was the lowest for C followed by B samples, result attributed to the more uniform and compact morphology of C samples (Figures 1(b) and 1(c)). During the first hours of immersion, the  $Q_1$  values of C and B samples increased, being much more evident (two orders of magnitude) the corresponding to C samples. These changes, coupled to the  $n_1$  values evolution, can be explained assuming that despite the blockage of the fissures and pores of the conversion layer with the corrosion products, these last provides a poor dielectric behavior and, therefore, are unable to inhibit the corrosion process. For the first hours, A samples exhibited a trend to decrease the  $Q_1$  values followed by an increase of approximately one order of magnitude, which is indicative of conversion layer degradation [39]. The decreasing  $n_1$  values shown in Figure 6(b) for B and C samples may be interpreted as a trend to change from capacitive to diffusional behavior, or a mix of both. On the other hand, the A samples showed an opposite response [40]. After several hours of exposure, all these changes followed the observed for the  $Q_1$  values.

The analysis of  $R_2$  (charge transfer resistance) as a function of immersion time is a useful tool for the corrosion rate evaluation since it gives information about the kinetic of the corrosive process. In such sense, Figure 7 shows that according to the equivalent circuit utilized for fitting the impedance data (Figure 4(b)), C samples did not present the time constant ( $R_2Q_2$ ) corresponding to the faradaic process. It means that this type of conversion layer provided barrier properties (Figure 5) high enough as to inhibit the corrosion process throughout the test. On the other hand, the fact that the  $R_2$  values were greater for B samples than for A samples means that those showed lower corrosion rates. This was attributed to the fact that

the zinc corrosion products gathered in the conversion layer defects acted as a better partial barrier, but also that such an effect disappeared as the time of exposure elapsed.

This analysis of EIS data for the three Cr<sup>3+</sup>-based conversion treatments showed that a deficient deposition of the conversion layer produces coatings with lower barrier properties and, therefore, lower corrosion protection (as particularly found in the case of A samples).

Summarizing, green-colored Cr<sup>3+</sup> passivation exhibited higher protective capacity than yellow-colored Cr<sup>3+</sup> and blue-colored Cr<sup>3+</sup> passivation layers, which is clearly noted in the polarization curves data (Figure 2).

#### 4. Conclusions

From the results generated during this investigation for three alternative conversion treatments applied on electrogalvanized steel, the following conclusions can be made with regard to their corrosion performance in contact with a chloride solution at room temperature:

- the more uniform coating presented lower corrosion rate;
- the electrochemical techniques demonstrated to be a very useful tool to characterize the corrosion protection provided by different conversion treatments;
- the EIS data analyses based on equivalent circuit models showed that green-colored Cr<sup>3+</sup> conversion treatment (C samples) presented the highest corrosion protection followed by the yellow-colored Cr<sup>3+</sup> conversion treatment (B samples) and blue-colored Cr<sup>3+</sup> conversion treatment (A samples), respectively. This behavior was in agreement with the results obtained of the polarization curves;
- the conversion treatments investigated shown interesting results but other experiments need to be performed in order to evaluate alternatives to the traditional and highly effective, but toxic and pollutant, Cr<sup>6+</sup> based conversion treatment.

In the near future it is likely that stringent legislation will require the total removing of hexavalent chromium as anticorrosive treatment. Consequently, more studies are needed concerning the corrosion protection, ecological and toxic effects afforded by new alternative treatments.

#### 5. Acknowledgements

The authors acknowledge CNPq/PROSUL (Process 490 116/2006-0) of Brazil, CAPES/MINCyT (Process 158/09 of Brazil and BR/08/04 of Argentina), and Comisión de Investigaciones Científicas de la Provincia de Buenos Aires (CIC) and Consejo Nacional de Investigaciones Científicas y Técnicas (CONICET) of Argentina by their

financial support to this research.

## REFERENCES

- [1] N. Zaki, "Chromate Conversion Coating for Zinc," *Metal Finishing*, Vol. 86, No. 2, February 1988, pp. 75-78.
- [2] P. L. Hagans and C. M. Haas, "ASM Handbook," *Surface Engineering, ASM International*, Vol. 5, 1994.
- [3] F. Deflorian, S. Rossi, L. Fedrizzi and P. L. Bonora, "EIS Study of Organic Coating on Zinc Surface Pretreated with Environmentally Friendly Products," *Progress in Organic Coatings*, Vol. 52, No. 4, 2005, pp. 271-279.
- [4] R. Berger, U. Bexell, T. M. Grehk and S. E. Hörnström, "A Comparative Study of the Corrosion Protective Properties of Chromium and Chromium Free Passivation Methods," *Surface and Coatings Technology*, Vol. 202, No. 2, 2007, pp. 391-397.
- [5] K. W. Cho, V. S. Rao and H. Kwon, "Microstructure and Electrochemical Characterization of Trivalent Chromium Based Conversion Coating on Zinc," *Electrochimica Acta*, Vol. 52, No. 13, 2007, pp. 4449-4456.
- [6] Y.-T. Chang, N.-T. Wen, W.-K. Chen, M.-D. Ger, G.-T. Pan and T. C.-K. Yang, "The Effects of Immersion Time on Morphology and Electrochemical Properties of the Cr(III)-Based Conversion Coatings on Zinc Coated Steel Surface," *Corrosion Science*, Vol. 50, No. 12, 2008, pp. 3494-3499.
- [7] X. Zhang, C. Van den Bos, W. G. Sloof, A. Hovestad, H. Terry and J. H. W. de Wit, "Comparison of the Morphology and Corrosion Performance of Cr(VI)- and Cr(III)-Based Conversion Coatings on Zinc," *Surface and Coatings Technology*, Vol. 199, No. 1, 2005, pp. 92-104.
- [8] N. T. Wen, F. J. Chen, M. D. Ger, Y. N. Pan and C. S. Lin, "Microstructure of Trivalent Chromium Conversion Coating on Electrogalvanized Steel Plate," *Electrochemical Solid State Letter*, Vol. 11, No. 8, 2008, pp. C47-C50.
- [9] N.-T. Wen, C.-S. Lin, C.-Y. Bai and M.-D. Ger, "Structures and Characteristics of Cr(III)-Based Conversion Coatings on Electrogalvanized Steels," *Surface and Coatings Technology*, Vol. 203, No. 3-4, 2008, pp. 317-323.
- [10] B. Da Fonte, Jr. and M. C. Mich, US Patent 4.359.345, 1982.
- [11] C. R. Tomachuk, C. I. Elsner, A. R. Di Sarli and O. B. Ferraz, "Morphology and Corrosion Resistance of Cr(III)-Based Conversion Treatments Applied on Electrogalvanized Steel," *Journal of Coatings Technology and Research*, Vol. 7, No. 4, 2010, pp. 493-502.
- [12] C. R. Tomachuk, C. I. Elsner, A. R. Di Sarli and O. B. Ferraz, "Corrosion Resistance of Cr(III) Conversion Treatments Applied on Electrogalvanized Steel and Subjected to Chloride Containing Media," *Materials Chemistry and Physics*, Vol. 119, No. 1-2, 2009, pp. 19-29.
- [13] E. Almeida, T. C. Diamantino, M. O. Figueiredo and C. Sá, "Oxidizing Alternative Species to Chromium VI in Zinc Galvanized Steel Surface Treatment. Part 1. A Morphological and Chemical Study," *Surface and Coatings Technology*, Vol. 106, No. 1, July 1998, pp. 8-17.
- [14] E. Almeida, L. Fedrizzi and T. C. Diamantino, "Oxidizing Alternative Species to Chromium VI in Zinc Galvanized Steel Surface Treatment. Part 2. An Electrochemical Study," *Surface and Coatings Technology*, Vol. 105, No. 1-2, June 1998, pp. 97-101.
- [15] G. D. Wilcox and D. R. Gabe, "Passivation Studies Using Group VIA Anions. V. Cathodic Treatment of Zinc," *British Corrosion Journal*, Vol. 22, No. 4, 1987, pp. 254-258.
- [16] G. D. Wilcox, D. R. Gabe and M. E. Warwick, "The Development of Passivation Coatings by Cathodic Reduction in Sodium Molybdate Solutions," *Corrosion Science*, Vol. 28, No. 6, 1988, pp. 577-585, 587.
- [17] V. I. Korobov, Y. M. Loshkarev and O. V. Kozhura, "Cathodic Treatment of Galvanic Zinc Coatings in Solutions of Molybdates," *Russian Journal of Electrochemistry*, Vol. 34, No. 11, 1998, pp. 1154-1157.
- [18] P. D. Deck and D. M. Reichgott, "Characterization of Chromium-Free No-Rinse Prepaint Coatings on Aluminium and Galvanized Steel," *Metal Finishing*, Vol. 90, No. 9, 1992, pp. 29-35.
- [19] B. R. W. Hinton, "Corrosion Prevention and Chromates, the End of an Era?" *Metal Finishing*, Vol. 89, No. 9, 1991, pp. 55-61.
- [20] B. R. W. Hinton, "Corrosion Prevention and Chromates, the End of an Era?" *Metal Finishing*, Vol. 89, 1991, pp. 15-20.
- [21] A. Barbucci, M. Delucchi and G. Cerisola, "Study of Chromate-Free Pretreatments and Primers for the Protection of Galvanized Steel Sheets," *Progress in Organic Coatings*, Vol. 33, No. 2, 1998, pp. 131-138.
- [22] G. D. Wilcox and J. A. Wharton, "A Review of Chromate Free-Passivation Treatments for Zinc and Zinc Alloys," *Transactions of the Institute of Metal Finishing*, Vol. 75, No. 4, 1997, pp. B140-B146.
- [23] T. F. Child and W. J. van Ooij, "Application of Silane Technology to Prevent Corrosion of Metal and Improve Paint Adhesion," *Transactions of the Institute of Metal Finishing*, Vol. 77, No. 2, 1999, pp. 64-70.
- [24] S. González, M. A. Gil, J. O. Hernández, V. Fox and R. M. Souto, "Resistance to Corrosion of Galvanized Steel Covered with an Epoxy -Polyamide Primer Coating," *Progress in Organic Coatings*, Vol. 41, No. 1-3, March 2001, pp. 167-170.
- [25] M. F. Montemor, A. M. Simões, M. G. S. Ferreira and C. B. Breslin, "Composition and Corrosion Behavior of Galvanized Steel Treated with Rare-Earth Salts: The Effect of the Cation," *Progress in Organic Coatings*, Vol. 44, No. 2, 2002, pp. 111-120.
- [26] "Standard Practice for Operating Salt Spray (Fog) Apparatus," *ASTM B 117 Review A07*.
- [27] "Testing in a Saturated Atmosphere in the Presence of Sulphur Dioxide," DIN 50018, 1997.
- [28] "Atmospheres and their Technical Application Condensation Water Test Atmospheres," DIN 50017, 1982.
- [29] J. R. Mac Donald, "Impedance Spectroscopy Emphasiz-

- ing Solid State Materials,” John Wiley & Sons, New York, 1987.
- [30] F. Mansfeld, “Models for the Impedance Behavior of Protective Coatings and Cases of Localized Corrosion,” *Electrochimica Acta*, Vol. 38, No. 14, 1993, pp. 1891-1897.
- [31] P. Carbonini, T. Monetta, L. Nicodemo, P. Mastronardi, B. Scatteia and F. Bellucci, “Electrochemical Characterization of Multilayer Organic Coatings,” *Progress in Organic Coatings*, Vol. 29, No. 1-4, 1996, pp. 13-20.
- [32] L. de Rosa, T. Monetta, D. B. Mitton and F. Bellucci, “Monitoring Degradation of Single and Multilayer Organic Coatings. I. Absorption and Transport of Water: Theoretical Analysis and Methods,” *Journal of the Electrochemical Society*, Vol. 145, No. 11, 1998, pp. 3830-3838.
- [33] A. Boukamp, “Equivalent Circuit,” Report CT88/265/128, CT89/214/128, University of Twente, The Netherlands, 1989.
- [34] N. M. Martyah and J. E. McCaskie, “Corrosion Behavior of Zinc Chromate Coatings,” *Metal Finishing*, Vol. 94, No. 2, 1996, pp. 65-67.
- [35] C. Delouis, M. Duprat and C. Tournillon, “The Kinetics of Zinc Dissolution in Aerated Sodium Sulphate Solutions. A Measurement of the Corrosion Rate by Impedance Techniques,” *Corrosion Science*, Vol. 29, No. 1, 1989, pp. 13-20.
- [36] B. Del Amo, L. Véleva, A. R. Di Sarli and C. I. Elsner, “Performance of Coated Steel Systems Exposed to Different Media. Part 1: Painted Galvanized Steel,” *Progress in Organic Coatings*, Vol. 50, No. 3, 2004, pp. 179-192.
- [37] E. P. M van Westing, G. M. Ferrari, F. M. Geenen and J. H. W. de Wit, “In Situ Determination of the Loss of Adhesion of Barrier Epoxy Coatings Using Electrochemical Impedance Spectroscopy,” *Progress in Organic Coatings*, Vol. 23, No. 1, 1993, pp. 89-103.
- [38] G. G. Nascimento, O. R. Mattos, J. L. C. Santos and I. C. P. Margarit, “Impedance Measurements on Lacquered Tinplate: Fitting with Equivalent Circuits,” *Journal of Applied Electrochemistry*, Vol. 29, No. 3, March 1999, pp. 383-392.
- [39] F. Mansfeld, “Use of Electrochemical Impedance Spectroscopy for the Study of Corrosion Protection by Polymer Coatings,” *Journal of Applied Electrochemistry*, Vol. 25, No. 3, March 1995, pp. 187-202.
- [40] R. L. Zeller and R. F. Savinell, “Interpretation of AC Impedance Response of Chromated Electrogalvanized Steel,” *Corrosion Science*, Vol. 26, No. 5, 1986, pp. 389-399.